Combining Computational Modeling with Reaction Kinetics Experiments for Elucidating the *In Situ* Nature of the Active Site in Catalysis

Saurabh Bhandari, Srinivas Rangarajan,† Manos Mavrikakis*

Department of Chemical and Biological Engineering, University of Wisconsin-Madison, Madison, WI 53706, USA

* corresponding author emavrikakis@wisc.edu

CONSPECTUS

Microkinetic modeling based on density functional theory (DFT) derived energetics is important for addressing fundamental questions in catalysis. The quantitative fidelity of microkinetic models (MKMs), however, is often insufficient to conclusively infer the mechanistic details of a specific catalytic system. This can be attributed to a number of factors such as an incorrect model of the active site for which DFT calculations are performed, deficiencies in the hypothesized reaction mechanism, inadequate consideration of the surface environment under reaction conditions, and the intrinsic errors in the DFT exchange-correlation functional. Despite these limitations, we aim at developing a rigorous understanding of the reaction mechanism and of the nature of the active site for heterogeneous catalytic chemistries under reaction conditions. By achieving parity between reaction kinetics experimental outcomes and modeling outcomes through robust parameter estimation and by ensuring coverage-consistency between DFT calculations and MKM predictions, it is possible to systematically refine the mechanistic model and, thereby, our understanding of the catalytic active site *in situ*.

Our general approach consists of developing *ab initio*-informed MKM for a given active site and then re-estimating the energies of the transition and intermediate states so that the model predictions match quantities measured in reaction kinetics experiments. If: (i) model-experiment parity is high, (ii) the adjustments to the DFT-derived energetics for a given model of the active site are rationalized within the errors of standard DFT exchange-correlation functionals, and (iii) the resultant MKM predicts surface coverages that are consistent with those assumed in the DFT calculations used to initialize the MKM, we conclude that we have correctly identified the active site and the reaction mechanism. If one or more of these requirements are not met, we iteratively refine our model by updating our hypothesis for the structure of the active site and/or by incorporating coverage effects, until we obtain a high-fidelity coverage-self-consistent MKM whose final kinetic and thermodynamic parameters are within error of the values derived from DFT.

Using the catalytic reaction of formic acid (FA, HCOOH) decomposition over transition-metal catalysts as an example, here we provide an account of how we applied this algorithm to study this chemistry on powder Au/SiC and Pt/C catalysts. For the case of Au catalysts, on which the FA decomposition occurred exclusively through the dehydrogenation reaction ($HCOOH \rightarrow CO_2+H_2$), our approach was used to iteratively refine the model starting from the (111) facet until we found that specific ensembles of Au atoms present in sub-nanometer clusters can describe the active site for this catalysis. For the case of Pt catalysts, wherein both dehydrogenation ($HCOOH \rightarrow CO_2+H_2$) and dehydration ($HCOOH \rightarrow CO+H_2O$) reactions were active, our approach identified that a partially CO*-covered (111) surface serves as the active site and that CO*-assisted steps contributed substantially to the overall FA decomposition activity. Finally, we suggest that once

the active site and the mechanism are conclusively identified, the model can subsequently serve as a high-quality basis for designing specific goal-oriented experiments and improved catalysts.

KEY REFERENCES

- Singh, S.; Li, S.; Carrasquillo-Flores, R.; Alba-Rubio, A. C.; Dumesic, J. A.; Mavrikakis, M. Formic Acid Decomposition on Au Catalysts: DFT, Microkinetic Modeling, and Reaction Kinetics Experiments. *AIChE J.* **2014**, *60*, 1303–1319.[1] This study utilizes a combined approach involving DFT, reaction kinetics experiments, and mean-field microkinetic modeling to point to the role of coordinatively unsaturated sites in catalyzing FA decomposition on Au/SiC.
- Li, S.; Singh, S.; Dumesic, J. A.; Mavrikakis, M. On the Nature of Active Sites for Formic Acid Decomposition on Gold Catalysts. *Catal. Sci. Technol.* **2019**, *9*, 2836–2848.[2] In this study, DFT-derived mean-field microkinetic models were utilized to investigate FA decomposition on unsupported subnanometric Au clusters (Au_2-Au_{25}), identifying Au_{18} as the most likely active species on Au/SiC catalysts.
- Chen, B. W. J.; Stamatakis, M.; Mavrikakis, M. Kinetic Isolation between Turnovers on Au18 Nanoclusters: Formic Acid Decomposition One Molecule at a Time. *ACS Catal.* **2019**, *9*, 9446–9457.[3] This study combined DFT with on-lattice kinetic Monte Carlo simulations to identify a pair of adjacent triangular ensembles as the active site for FA decomposition on Au_{18} clusters.
- Bhandari, S.; Rangarajan, S.; Maravelias, C. T.; Dumesic, J. A.; Mavrikakis, M. Reaction Mechanism of Vapor-Phase Formic Acid Decomposition over Platinum Catalysts: DFT, Reaction Kinetics Experiments, and Microkinetic Modeling. *ACS Catal.* **2020**, *10*, 4112–4126.[4] In this study, an iterative methodology involving DFT, reaction kinetics experiments, and mean-field microkinetic modeling, was utilized to derive a coverage self-consistent description for the active site of FA decomposition on Pt/C.

INTRODUCTION

MKMs formulated using energetics derived from DFT calculations are frequently employed to elucidate the underlying reaction mechanism of heterogeneously catalyzed reactions. **Figure 1** shows a schematic for an algorithm reflecting the workflow for microkinetic modeling based analysis that is typically employed in the catalysis literature, viz. – (i) enumerating the elementary steps in the reaction mechanism, (ii) using DFT to evaluate binding energies for each intermediate and transition-state energies for each elementary step, on an hypothesized structure of the catalytically-active site, (iii) formulating a MKM, which is a system of differential-algebraic equations within the mean-field approximation, with DFT computed parameters for kinetics (activation energies and pre-exponential factors) and thermochemistry, and (iv) solving the model to obtain information on the catalytic chemistry, including reaction rates, flux-carrying pathways, selectivity, apparent activation energy barriers, reaction orders, and rate-/selectivity-determining steps.

Being entirely *ab initio*, these models are in principle predictive and serve to bridge the gap between atomic-scale information (i.e., energies corresponding to most stable structures of intermediates and transition-states on a certain structure of the active site) and macroscopic observables (e.g., conversion and selectivity).[5–7] MKMs have often complemented experiments (microscopy, spectroscopy, and reaction kinetics experiments) to offer comprehensive insights into the reaction mechanism over a wide range of experimental conditions.[8,9] These insights can then serve as the basis for identifying new material compositions and atomic-scale architectures with improved catalytic activity and/or selectivity.[10–12]

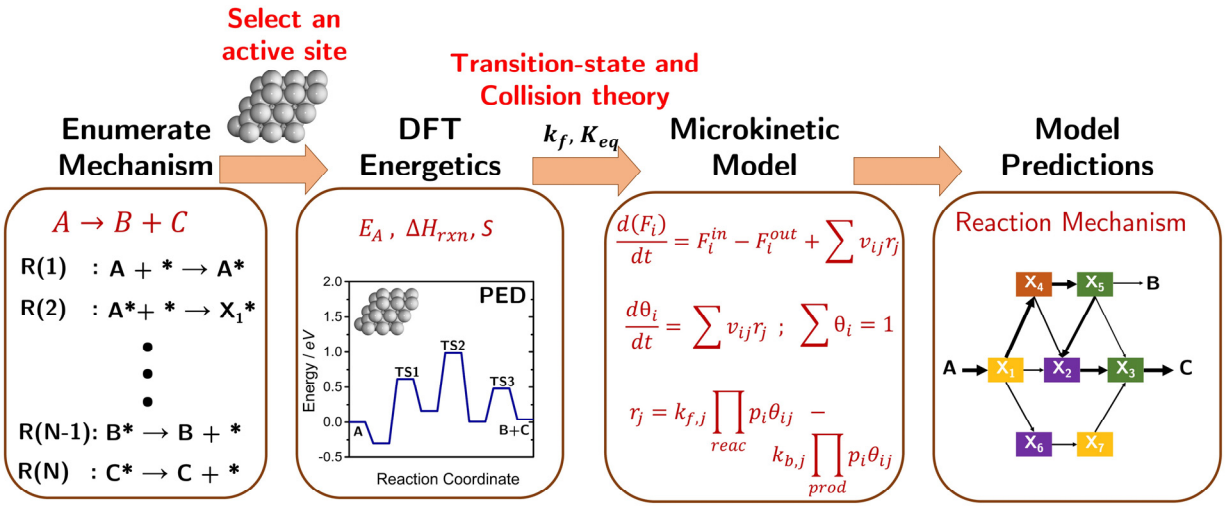

Figure 1: Schematic representation of the typical workflow adopted in a microkinetic-modeling (MKM)-based analysis for heterogeneous catalysis. '*A*', '*B*'/'*C*', and 'X_i's refer to reactant, products, and reaction intermediates, respectively. PED refers to potential energy diagram. Reactor balance equations (system of differential-algebraic equations) solved in a MKM are shown in the third panel.

A major caveat of the current approach (**Figure 1**) is that while these models often capture qualitative reactivity trends across experimental conditions and catalytic materials,[6,13,14] their quantitative accuracy vis-à-vis reaction kinetics experiments is often lacking. Indeed, the mismatch in reaction rates between model predictions and experiments can be several orders in magnitude and could stem from a number of factors,[1,15] such as : (1) an incomplete/incorrect reaction mechanism, (2) an active site model for which DFT energies are calculated, which is not dominating the catalytic action, (3) lack of consideration of surface environment effects, i.e., adsorbate-induced coverage-effects (clean-surface vs. a surface partially covered by spectators/reactants/products), and (4) the intrinsic limitations of standard DFT exchange-correlation functionals which are used to calculate the energetics.

A pertinent question arises: *Given this lack of fidelity, how can we identify active sites and reaction mechanism with a high degree of confidence?* To address this question, it is common to simply

adjust the kinetic and thermochemical parameters, to achieve model-experiment parity.[16–19] This parameter adjustment is often rationalized based on qualitative intuition such as: (i) the idealized models may not fully capture the complexity of the real catalyst, (ii) standard DFT functionals (PBE/PW91) overpredict the binding of covalently-bound small intermediates, whereas they underpredict the binding of larger intermediates (due to inadequate treatment of dispersive interactions),[20–22] and (iii) most common functionals perform poorly in predicting gas-phase energetics.[20,23,24] We have performed such adjustments through parameter estimation previously, however, we suggest that this approach represents only a partial solution to the problem of parity between measured and model predicted rates. While the resulting model might offer good predictive power, it does not necessarily provide a conclusive picture of the underlying reaction mechanism and of the nature of the active site. This is because: (i) there may be multiple solutions to the parameter estimation problem, (ii) the adjustments to the DFT-derived parameters may be too large to be easily rationalized, i.e., larger than the statistical-error of ~0.2 eV for the common GGA functionals (eg. PBE/PW91),[20,25–27] and (iii) the predicted surface coverage of various species could be dramatically different from the coverage assumed to compute the DFT energetics.

Here, we provide an account of the methodology developed in our group for formulating high-fidelity MKMs.[1–4,19,28–32] Specifically, we present our algorithmic approach for identifying active sites and reaction mechanisms in the context of the formic acid (FA) decomposition reaction (Scheme 1) – a chemistry which we have studied extensively, both computationally and experimentally – on supported Au[1–3] and Pt[4] catalysts (details regarding our assumptions and reaction engineering aspects of our MKM can be found in the corresponding references). Through these examples, we strive to convey the advantages of a systematic and integrated approach of

combining DFT calculations, reaction kinetics experiments, and microkinetic modeling to iteratively refine the atomic-scale picture of the active site and the reaction mechanism.

$$HCOOH \rightarrow H_2 + CO_2 \quad \text{(Dehydrogenation)} \quad ; \quad \Delta G\ (298\ K) = -43.5\ kJ/mol$$

$$HCOOH \rightarrow H_2O + CO \quad \text{(Dehydration)} \quad ; \quad \Delta G\ (298\ K) = -14.8\ kJ/mol$$

Scheme 1: Formic acid (FA, HCOOH) decomposition reactions. Gibbs free energies (ΔG) are calculated using the NIST thermochemistry database.[33]

FA DECOMPOSITION ON SUPPORTED GOLD CATALYSTS

Ojeda and Iglesia reported that finely-dispersed Au/Al_2O_3 catalysts decompose FA to H_2 selectively and exhibit higher activities compared to Pt catalysts,[34] one of the most active monometallic catalysts for FA decomposition.[35–37] These authors proposed that small Au clusters on Al_2O_3, undetected by transmission electron microscopy (TEM), were likely responsible for the exceptional catalytic activity.[34] Others have since corroborated that well-dispersed Au catalysts on a host of supports (SiC,[1] SiO_2,[38] ZrO_2,[39,40] CeO_2,[39,41] and TiO_2[42]) also exhibit high activity and high H_2 selectivity for FA decomposition. Although there is a consensus among these experimental studies that smaller Au nanoparticles or clusters are responsible for the remarkable FA decomposition reactivity of Au catalysts, the precise nature of the active site remained unknown. In the following, we describe our efforts to identify the nature of the active site for FA decomposition on Au/SiC using an algorithm that significantly expands on the approach outlined in **Figure 1**.

Iterative approach for elucidating the nature of the active site for FA decomposition on Au/SiC

We started with studying this catalysis by combining DFT, microkinetic modeling, and reaction kinetics experiments over Au/SiC.[1] Specifically, we proposed an algorithmic workflow, wherein we take input from reaction kinetics experiments and iteratively refine our computational models

to identify the nature of the active site (**Figure 2**). Accordingly, we initialized this procedure by hypothesizing a model for the active site, followed by: (i) evaluating DFT energetics to formulate a mean-field MKM, (ii) utilizing reaction kinetics experiments to systematically adjust DFT energetics to minimize model-experiment mismatch, (iii) evaluating if the parameter adjustments are rationalized within error of the exchange-correlation functional; if yes, we conclude that our hypothesis is correct, else, we utilize the insights gained from the parameter adjustment procedure to refine our hypothesis for the nature of the active site and re-perform this analysis iteratively until adjustments to DFT energetics are within the error of the functional. It is only then that we conclude that we have developed a reasonable vision for the nature of the active site.

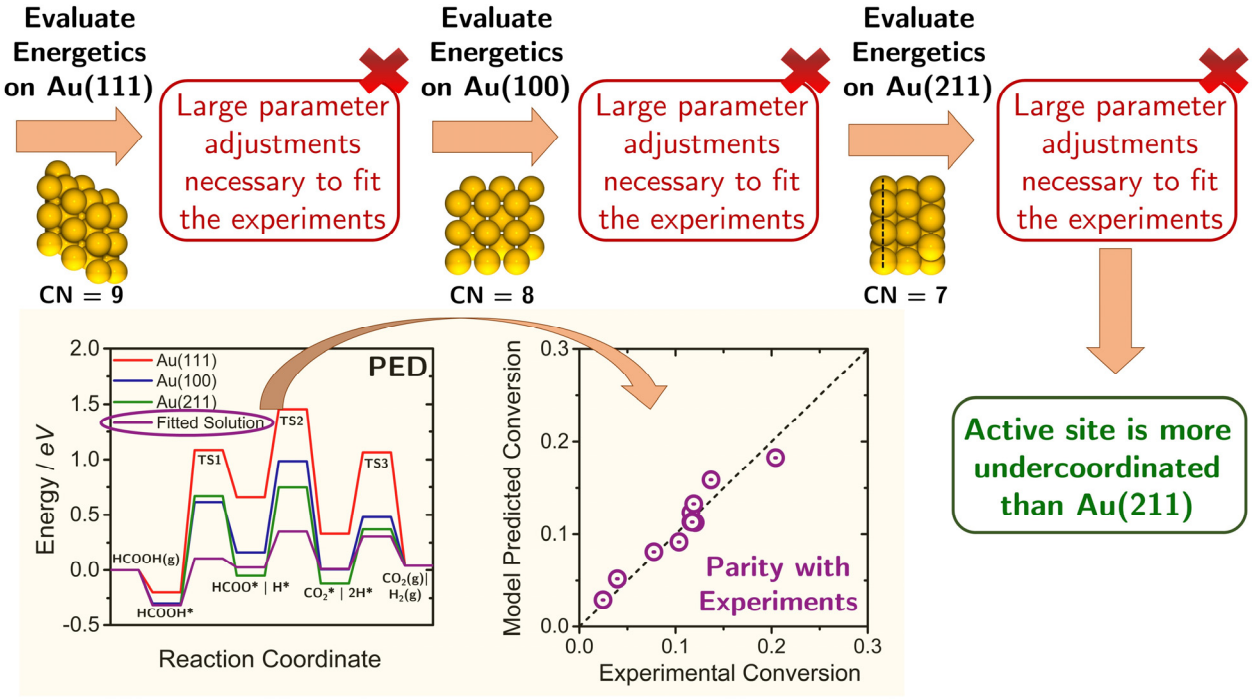

Figure 2: An iterative approach for elucidating the structure of the active site for FA decomposition on Au/SiC (ref. [1]). Feedback from parameter adjustment, required to fit the experiments (steady-state, <20% conversion, 1-4% FA, 0-6% H_2/CO_2, 343-383K; catalyst surface-site density determined from scanning transmission electron microscopy), is used to continually revise the hypothesis for the active site: Au(111)→Au(100)→Au(211). To fit the reaction kinetics experimental measurements, for all three facets (shown in the potential energy diagram (PED)), large parameter adjustments were necessary, indicating that the active site is more undercoordinated than Au(211). CN refers to surface coordination number. Vertical dashed black-line in the inset for Au(211) marks the step edge.

We started by considering the close-packed Au(111) facet (surface coordination number (CN) of 9) as the hypothesized model for the active site (**Figure 2**) and evaluated the energetics of a comprehensive reaction network comprising of 17 reaction steps and 15 distinct species, using plane-wave periodic DFT (PW91-GGA). We used zero-point energy (ZPE) corrected energetics to obtain initial estimates for the rate parameters used in the MKMs. However, the model significantly underpredicted the reaction rates compared to our experimental measurements. To fit the model-predicted rates with experimental rates, the energies of the transition-states and reaction intermediates had to be substantially modified (by as large as 1 eV). Such adjustments cannot be justified on the basis of GGA errors alone, and since a detailed reaction mechanism was modeled, we concluded that Au(111) cannot represent the active site for this chemistry. Nevertheless, the parameter adjustments needed for the MKM on Au(111) to capture the experimental data provided valuable guidance in searching for an alternative model for the active site. We noted that all the intermediates and transition-states had to be stabilized, suggesting that a more under-coordinated model site would potentially represent the active site better. Algorithmically (**Figure 2**), this led us to evaluate Au(100) (CN=8) and then Au(211) (CN=7) as plausible active sites. However, since large parameter adjustments were necessary on these two facets as well, we concluded that none of the facets explored yet were a good representation of the active site on Au/SiC.

The results showed that upon going from Au(111)→Au(100)→Au(211), the magnitude of the parameter adjustments progressively decreased, but all states still had to be further stabilized to rationalize the experimental reaction rates. These observations suggest that the active site might be more undercoordinated than Au(211) (CN<7), which would potentially stabilize the energetics for the intermediates and transition-states to an even greater extent, compared to Au(111), Au(100), and Au(211). Additionally, for all three models, >0.95 ML of the sites were predicted to

be vacant under all reaction conditions, which precludes any potential stabilizations stemming from adsorbate-adsorbate interactions.

Experimental insight on the catalytic active site for FA decomposition on Au/SiC

To further explore the role of undercoordinated Au sites, we synthesized Au catalysts with varying dispersion (average particle size ranging from 2.5-10.7 nm) and evaluated those through reaction kinetics experiments.[1] The results indicated that the turnover frequency (TOF) decreased with increasing average particle size, demonstrating the structure sensitivity of FA decomposition on Au/SiC. Subsequently, we estimated the fraction of various surface sites (corner, perimeter, terrace) as a function of particle size,[43–46] and concluded that the reaction rate correlated well with the number of corner sites. This conclusion based on experiments is in agreement with the insight gained from DFT-derived MKMs suggesting that indeed low-coordinated Au sites are playing a key role in FA decomposition.

FA decomposition on unsupported Au clusters

Motivated by this conclusion, we studied the role of low-coordinated sites in catalytically relevant sub-nanometric regimes. Specifically, we analyzed FA decomposition reaction paths on unsupported subnanometric Au clusters (up to Au_{25}~0.85nm), identified using *ab initio* molecular dynamics simulations.[2] To select the clusters characterized by energetics that could rationalize the experimental reaction rates, we used the activation energy barrier for the first FA dehydrogenation step (HCOOH* $\leftrightarrow$ HCOO*+H*) as a screening criterion (**Figure 3**). As Au(211), the most reactive of the three extended surfaces considered, predicted reaction rates that were 5-6 orders of magnitude smaller than the experimental reaction rates, the active clusters in the Au/SiC catalysts used in experiments should at least have a smaller activation energy barrier for FA dehydrogenation compared to that on Au(211).

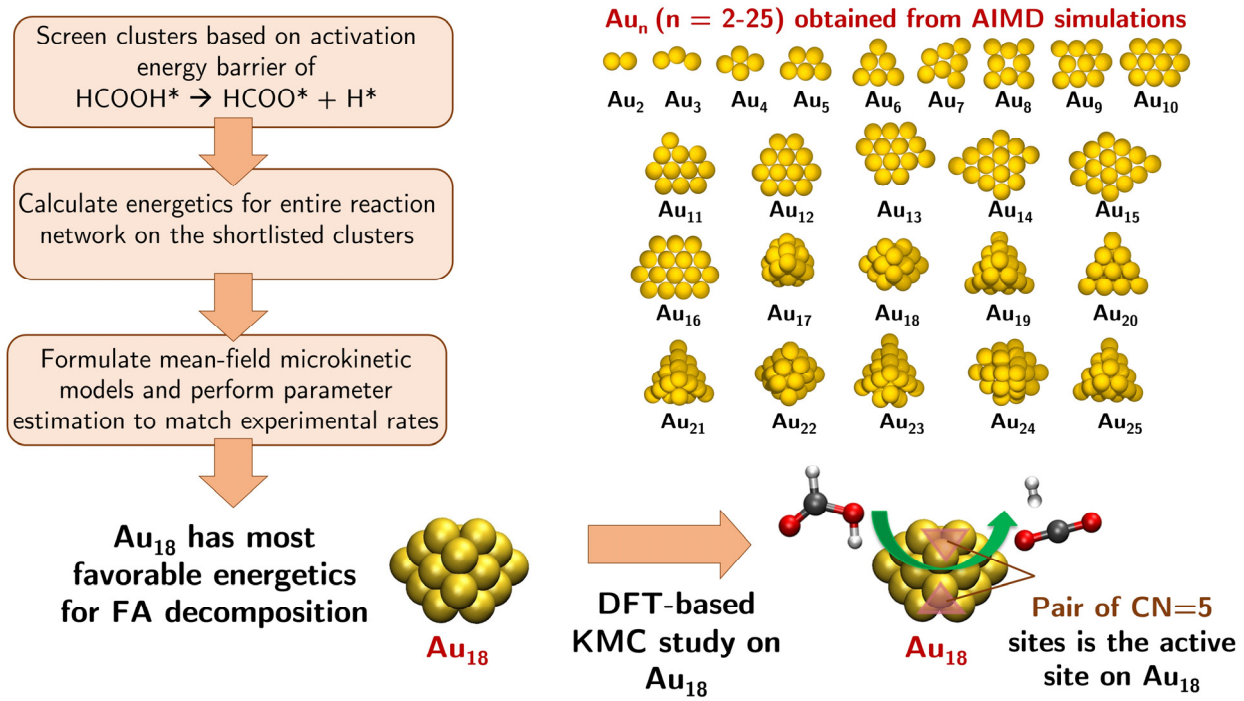

Figure 3: Elucidating the active site for FA decomposition on unsupported subnanometric Au clusters (ref. [2]). Most stable geometries of Au_n (n=2-25) clusters (<0.85nm) obtained from *ab initio* molecular dynamics (AIMD) are shown. Combination of DFT-derived mean-field MKMs and reaction kinetics experiments on Au/SiC, led to the conclusion that Au_{18} might resemble the active site the best. Kinetic Monte Carlo (KMC) study on Au_{18} revealed that a pair of adjacent Au_3 ensembles (coordination number (CN) of 5), can be the active site for FA decomposition on Au/SiC (ref. [3]).

Consequently, we performed detailed reaction pathway studies on the shortlisted subset of clusters (Au_4, Au_5, Au_7, Au_{17}, Au_{18}, and Au_{19}), which were identified as potential candidates for the active site on Au/SiC. Mean-field MKMs were then developed using the DFT energetics calculated for these clusters and were subsequently fit to the experimental data through parameter adjustment. This entire process (**Figure 3**) identified the Au_{18} cluster to possess the most favorable energetics, requiring only minimal parameters adjustments to fit the experimental data.

Although, mean-field MKMs provide valuable information to guide the search of active site geometry, subnanometric clusters such as the catalytically active Au_{18}: (i) offer a spatially inhomogeneous surface, (ii) present discrete adsorbate coverages, and (iii) lead to strong adsorbate

interactions due to quantum-size effects and superatomic nature of the clusters.[3,47] These properties mandate the use of methods that better capture local effects. In a recent study,[3] we combined DFT calculations with cluster-expansion[48,49] and on-lattice kinetic Monte Carlo (KMC) simulations[50,51] to derive a rigorous mechanistic description for FA decomposition on Au_{18} clusters. The results suggest that a pair of adjacent Au_3 triangular ensembles (CN=5) is likely the active site for FA decomposition on Au_{18} clusters. Dissociation of a single FA molecule, leads to the simultaneous occupation of each of these triangular-sites by HCOO* and H*, which in turn results into a strong stabilization of the Au_{18} cluster. This stabilization prevents dehydrogenation of a second FA molecule, until the first molecule is fully decomposed to CO_2(g) and H_2(g). In other words, Au_{18} processes one FA molecule at a time, thereby explaining the kinetic isolation of decomposition events associated with the exclusive HD production observed in experiments with half-deuterated FA molecules over Au/Al_2O_3.[34] The reaction occurs through the HCOO*-mediated pathway ($HCOOH^* \leftrightarrow HCOO^*+H^* \leftrightarrow CO_2^*+2H^* \leftrightarrow CO_2+H_2$) with complete selectivity towards H_2, which rationalizes the experimentally observed selectivity towards dehydrogenation on Au/SiC. Dehydrogenation of HCOO* carries the highest degree of rate control[52] for all conditions and is therefore the rate-determining step.

In the case of FA decomposition over Au/SiC, we showed that the mechanism and active site (pair of Au_3 sites on Au_{18}) could not have been identified following the approach described in **Figure 1**. Further, we demonstrated that finding an accurate active site model alone through parameter adjustments, is insufficient. Only an active site model that yields a high degree of parity with experimental measurements and whose parameter adjustments are within the error of the utilized functional, offers a desirable stopping point for the active site identification algorithm. It is only at that point we can extract reliable mechanistic insights.

FA DECOMPOSITION ON SUPPORTED PLATINUM CATALYSTS

Experimental studies demonstrate Pt as one of the most active monometallic catalysts for FA decomposition.[35–37] Unlike Au catalysts which selectively dehydrogenates FA, both the dehydrogenation (CO_2+H_2) and dehydration (CO+H_2O) pathways are active on Pt, with >95% selectivity towards dehydrogenation.[37,53] Additionally, formation of CO as one of the decomposition products implies the presence of adsorbed CO (CO*) on the catalyst surface, leading to the well-known problem of CO*-poisoning of Pt catalysts.[37,54] Despite numerous computational and experimental studies of this reaction, the nature of surface reaction intermediates along with their abundance, the reaction mechanism, and the nature of the active site as a function of reaction conditions, have not been elucidated. Herein, we discuss our algorithmic approach for addressing these fundamental questions for FA decomposition on Pt/C (**Figure 4**).[4]

Iterative approach for elucidating the active site for FA decomposition on Pt/C

We started by considering extended clean Pt(100) and Pt(111) surfaces as the active site model and calculated the energetics (DFT-PW91-GGA) for a comprehensive reaction network involving 25 elementary steps and 20 species. To incorporate ZPE and temperature–corrected DFT energetics in our mean-field MKMs, we derived Shomate parameters,[33] using vibrational frequency calculations and statistical mechanics. Both clean (111) and (100) models, however, predicted reaction rates that were several orders of magnitude lower than our experimental rates (steady-state, <10% conversion, 1-5% FA, 0-10% H_2/CO_2, 0-0.1% H_2O/CO, 358-378 K; catalyst surface-site density determined from CO chemisorption). Next, we performed parameter estimation to determine the adjustments on the two surfaces that would yield quantitative agreement with our experimental data.

Post parameter adjustments, both clean Pt(111) and Pt(100) demonstrated improved agreement with experimental measurements. However, these models were found to be inadequate representations of the active site on Pt/C, since they: (i) failed to reproduce rates when CO was co-fed in the reactor, (ii) predicted high coverage of CO* (>0.90 ML, averaged over all experiments), inconsistent with the clean-surface assumption at which the DFT energetics were calculated, and (iii) required large adjustments to the DFT-derived activation energy barriers for several elementary steps, well beyond the typical GGA errors (**Figure 4**). Although these models fell short in explaining the experiments, their analysis provided useful insights regarding the nature of the most abundant surface intermediate (MASI) under experimental conditions, viz. CO*. In principle, one could also validate this model prediction using *operando* spectroscopy. Indeed, there is ample spectroscopic evidence (*in situ* Fourier-transform infrared spectroscopy (FTIR)) for partial CO*-poisoning of supported Pt catalysts, under typical FA decomposition conditions.[37,54] Motivated by these insights, we updated our hypothesis for the active site model and, in the next step, considered partially CO*-covered (111) and (100) facets (**Figure 4**), thereby explicitly accounting for CO* coverage-effects.

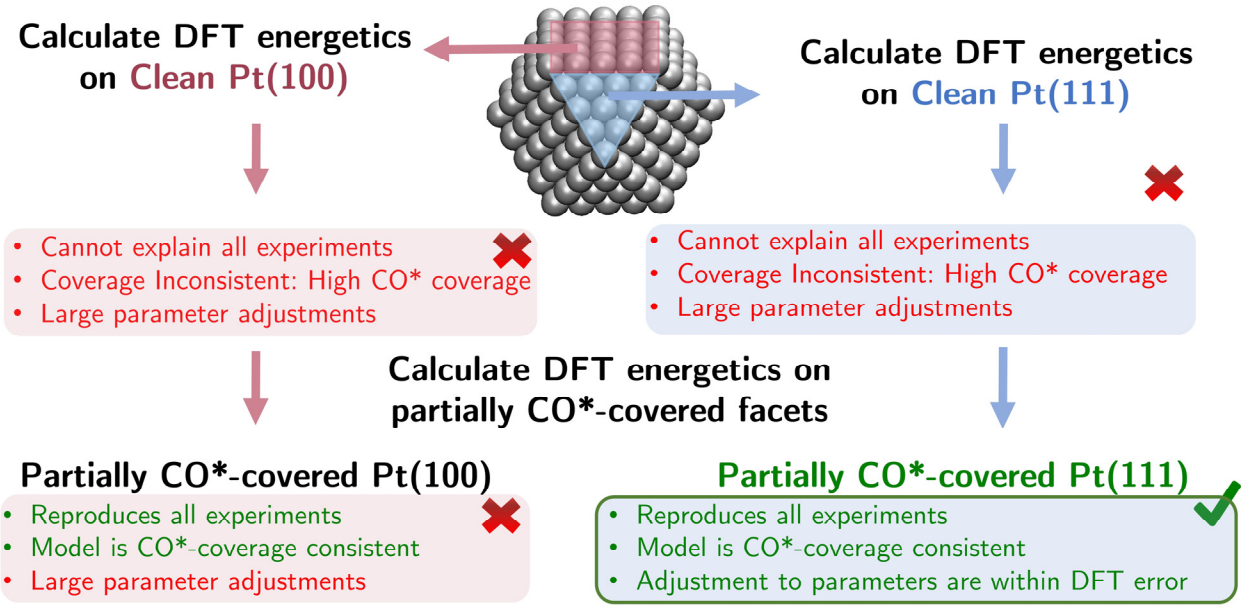

Figure 4: Workflow for developing a coverage self-consistent description of the active site for FA decomposition on Pt/C (ref. [4]). Mean-field MKMs formulated using DFT energetics on clean Pt(100) and Pt(111) were found to poorly describe the active site. Feedback from the parameter estimation is used to iteratively update the hypothesis for the nature of the active site.

Modeling CO spectator-induced coverage-effects*

Consequently, using DFT, we reinvestigated the entire reaction network on partially (4/9 ML) CO*-covered Pt(100) and Pt(111) surfaces. The choice of 4/9 ML CO*, used as an initial estimate of the *in situ* coverage, was motivated by previous experimental determination of CO*-saturation coverages on Pt surfaces under low CO partial pressures, which is similar to that experienced by Pt/C under FA decomposition reaction conditions.[55] The presence of CO* on the catalyst surface opened new pathways, including CO*-assisted dehydrogenation steps, which were now included in the refined reaction network. In addition, we evaluated the reaction energetics (binding/transition-state energies) at varying CO*-coverage levels to determine the variation of the energetics as polynomial-functions of CO* coverage. The resultant polynomial-functions were

incorporated in our MKMs, thereby enabling CO* coverage-dependent energetics for the new models.

After parameter adjustments, both the *CO* coverage-cognizant* Pt(100) and Pt(111) models were able to accurately describe the experimental data, including the subset of the experiments with CO-co-feed, which were not well reproduced by our clean surface models. Furthermore, these MKMs predicted CO* coverages (~4/9 ML CO* on Pt(100); ~3/9 ML on Pt(111)) which were consistent with coverages of 4/9 ML CO* spectators used in the catalyst model for DFT calculations. Both these MKMs were therefore CO*-coverage *self-consistent*. Analysis of the parameter adjustments revealed that Pt(100) required large adjustments to the DFT calculated activation energy barriers (**Figure 4**). By constraining the adjustments to the typical GGA error of ±0.2 eV,[20,25–27,56,57] we found that Pt(100) was largely poisoned by CO* (~0.5 ML) and was rendered inactive under our reaction conditions. On the other hand, parameter adjustments required for the partially CO*-covered Pt(111) model were within GGA error. We therefore concluded that a partially CO*-covered Pt(111) accurately represents the active site for FA decomposition on Pt/C.

The MKM analysis revealed that on the partially CO*-covered Pt(111), the reaction proceeds through the COOH* mechanism (**Figure 5**). Both the direct COOH* dehydrogenation (COOH* $\leftrightarrow$ CO_2*+H*) and the CO*-spectator assisted dehydrogenation (COOH*+**<u>CO</u>*** $\leftrightarrow$ CO_2*+**<u>CO</u>**H***;*** CO*-spectators are denoted by **<u>CO</u>***) pathways contributed to the dehydrogenation reaction flux. These CO* spectator-assisted pathways were found to be essential for accurately reproducing the experimentally measured apparent activation energy barriers and reaction orders.

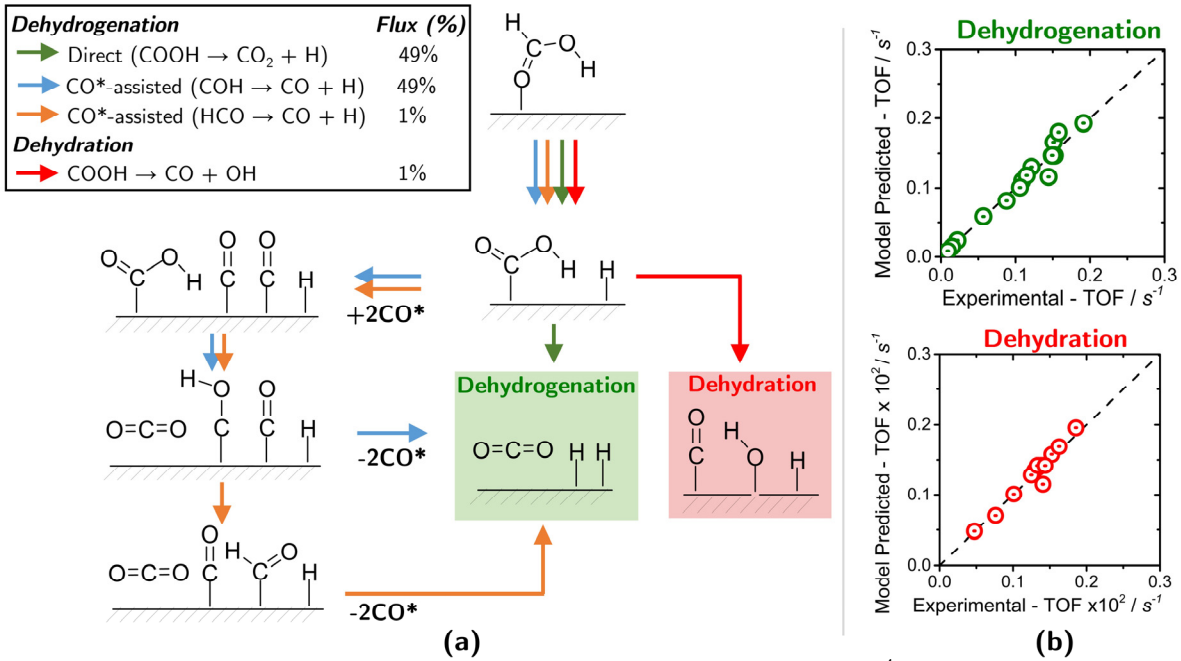

Figure 5: Results from the MKM on a 4/9 ML CO*-covered Pt(111) (ref. [4]): (a) Reaction mechanism for FA decomposition on Pt/C. Formate-mediated pathways were considered, but did not contribute significantly to FA decomposition. Flux contributions for the various pathways at 2.6% FA, balance He (1 atm, 373K) are indicated, (b) Parity plots comparing model-predicted and experimental turnover frequencies (TOFs).

This example speaks to the importance of practicing coverage self-consistent microkinetic modeling and of combining it with experimental data for elucidating the nature of active site and the reaction mechanism. Modeling CO* coverage-effects for this chemistry: (1) yielded improved initial estimates for the energetics used in the MKM, since these parameters required minimal adjustments to fit with the experiments and (2) inspired the consideration of CO* spectator-assisted pathways, which were essential in reproducing the experimental data. The traditional approach (**Figure 1**) was again insufficient; our iterative approach, however, revealed that accounting for CO* coverages was essential in determining both the active site and the reaction mechanism.

AN ALGORITHM TO IDENTIFY ACTIVE SITE AND REACTION MECHANISM

The process of iterative model refinement, employed in both examples, can be formalized as a general algorithm (**Figure 6**), which substantially expands on the conventional methodology shown in Figure 1. We initialize the algorithm with a hypothesized active site model, perform detailed reaction pathway studies using DFT, and formulate a MKM. We then incorporate data from reaction kinetics experiments and perform parameter estimation to achieve parity with the experiments. The optimized model is evaluated on the following three criteria: (i) Can the model accurately reproduce the experimental data?, (ii) Are the parameter adjustments needed to capture the experiments within error of the utilized exchange-correlation functional?, (iii) Is the model-predicted surface-environment consistent with the coverages at which the DFT energetics were calculated? If the optimized model satisfies all three criteria, we conclude that the hypothesized model for the active site accurately describes the nature of the active site. However, if even one of these criteria is not satisfied, we use insights gained from our parameter adjustment procedure to revise our hypothesis for the active site (i.e., active site geometric model, reaction mechanism, spectator coverage-effects), and reiterate all steps in the algorithm until all three criteria are met. The resultant high-fidelity model can then be used to perform well-educated reaction engineering tasks, e.g.: (i) predict behavior of the catalyst with quantitative accuracy (i.e., activity, selectivity, surface coverages, reaction mechanism, etc.), under other experimental conditions, (ii) perform experimental design with specific goals in mind: to identify experimental conditions for optimizing yield of product(s) or surface concentration of reaction intermediate(s), which, in turn, could enable spectroscopic identification of elusive reaction intermediates, and (iii) investigate related chemistries (e.g., the reverse reaction).

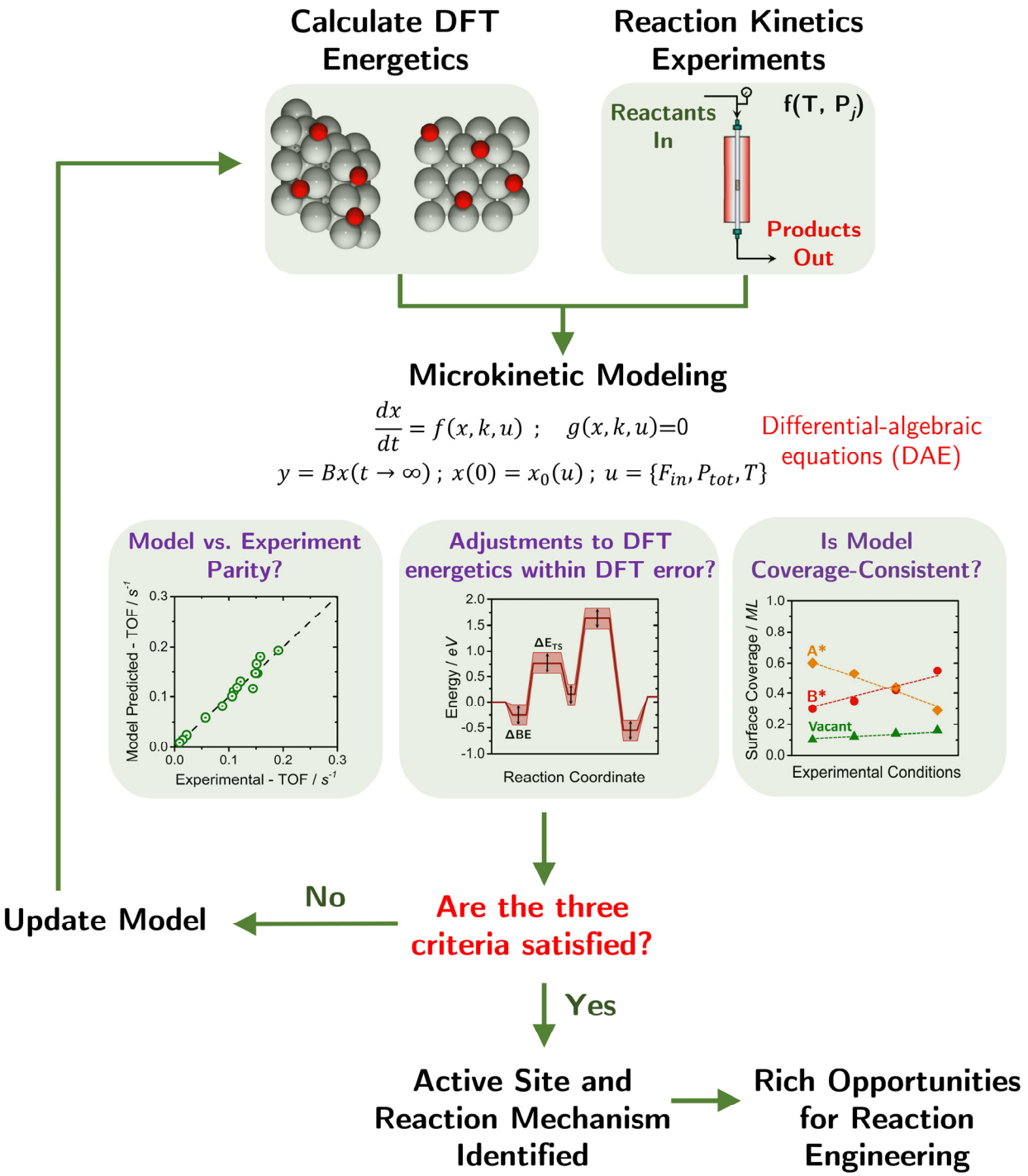

Figure 6: Proposed algorithmic scheme for elucidating the nature of the catalytic active site and the reaction mechanism, using a combination of DFT, reaction kinetics experiments, and microkinetic modeling.

PARAMETER ESTIMATION

A critical part of the algorithm is parameter estimation where we minimize the model-experiment mismatch (of TOFs) by adjusting the energetics of surface intermediates and transition-states from their respective DFT-values. Mathematically, this is a nonlinear optimization problem with the MKM (at different experimental conditions) as constraints. Solving this problem is challenging because: (i) the optimization problem is highly nonlinear due to the numerical stiffness of the MKM, (ii) we seek solutions where the insensitive parameters are automatically identified and set to zero (i.e., energy is set to the respective DFT value) to avoid overfitting, (iii) we require alternative solutions (minima) to compare potentially competing models. Accordingly, by leveraging modern numerical solvers and optimizers from the process systems engineering community,[58,59] we have developed two different approaches and tools to rigorously solve these parameter estimation problems[19,31] and to identify a comprehensive set of solutions meeting the convergence criteria of the algorithm. In both methods, we apply (i) a regularization penalty that ensures that the DFT-derived energetics are adjusted to the least possible extent, thereby, enhancing the credibility of the solution and (ii) a multi-start scheme using uniform sampling of the parameter space to elucidate plausible alternate solutions. Insights from benchmarking studies[20,60] regarding the uncertainty for the DFT energetics can inform the bounds on the maximum allowable adjustments for the DFT-energetics, thereby reducing the parameter space in which the search for acceptable solutions is conducted.

Alternate formulations, such as Bayesian parameter estimation, have also been employed, which incorporates errors from both theory and experiment to identify the maximum of the posterior distribution, to fit the experiments, rather than solving as an optimization problem.[27]

OUTLOOK

In **Figure 6**, we formalize our novel and comprehensive algorithm combining DFT, reaction kinetics experiments, and MKM to determine: (i) the nature of the active site in catalysis while the reaction is taking place and (ii) the detailed reaction mechanism for small-to-medium sized chemistries (~50 elementary steps). Selected opportunities for further methodological development are summarized here:

- *Errors in entropy*: In the parameter adjustment step of the algorithm, we have implicitly assumed that the errors arise in energies; not in entropy. While this assumption is reasonable when the intermediates are strongly bound (as in the examples discussed here), using standard quantum-harmonic approximations to estimate the partition function may grossly under-predict the entropy of weakly bound intermediates. [61–63] Further, inclusion of surface configurational entropy, associated with compensation effects in heterogeneous catalysis,[64–66] could also help improve the description of the active site. How these corrections/contributions can be included in our algorithm remains to be assessed.
- *Beyond monometallic catalysts and single-site models*: While our iterative algorithm is catalyst agnostic, its application to metal alloys, metal-support interfaces, oxide/sulfide-based catalysts, and materials with intrinsically isolated sites (e.g., zeolites, single-atom catalysts) has not yet been explored. For both examples here, single-site models seem adequate, indicating that only one site is at play. There may be catalytic systems wherein multiple sites are concurrently operative; in such cases, we expect that our algorithm will identify multiple plausible solutions, each corresponding to a contributing single-site. In those cases, we expect that the results of our analysis will inspire carefully designed additional experiments for further distinguishing contributions to reactivity by different sites.

- *Size-scalability:* Intrinsically complex reaction networks (comprising of hundreds of intermediates and thousands of reaction steps) routinely arise in catalysis (e.g., alkane reforming, hydrotreating, biomass upgrading, etc.); how this approach scales to such large reaction networks remains to be studied.
- *Assessing and improving the accuracy of first-principles calculations*: A number of recent functionals, e.g., PBE-D2/D3, opt-PBE, vdW-DF2, BEEF-vdW, etc., are now capable of better treating long-range dispersion interactions, which may contribute substantially to the interaction energies of large reaction intermediates.[67,68] Recent studies have also proposed systematic frameworks to analyze error propagation and to assess the uncertainty associated with MKM predictions, due to the errors stemming from the choice of DFT exchange-correlation functional.[26,69,70] Given their exorbitant computational cost, more accurate methods such as coupled cluster calculations, random-phase approximations, quantum Monte Carlo methods, etc. cannot yet be routinely applied in conjunction with MKM. However, advances in computing power and the recent development of approaches such as hybrid multi-level calculations[71] or quantum-mechanical embedding techniques[72,73] now allow for accurate calculation of a relatively small set of energies. The feasibility of infusing, perhaps selectively, such calculations to improve the model fidelity, represents an interesting research direction.
- *Beyond the mean-field approximation:* It is well-recognized that coverage-cognizant models offer a good trade-off between kinetic Monte Carlo and mean-field models in terms of accuracy and cost in treating coverage effects.[27] Recently, new approaches to obtain closed-form continuous functions relating the energetics and the coverage have been proposed which are nearly exact under the fast-diffusion limit.[74,75] The efficacy of these approaches within our algorithm remains to be explored.

Finally, we propose that our mathematically rigorous approach may have important implications for enhancing the fidelity of computational catalyst discovery approaches such as descriptor-based catalyst screening via higher-dimensional volcano plots. Conventionally this procedure entails: (i) evaluating the energetics of the reaction network on a 'reference' monometallic catalyst, (ii) extrapolating reaction energetics using the linear scaling[76] and Brønsted-Evans-Polanyi (BEP)[77] relationships, and (iii) elucidating reactivity trends across the descriptor space and identifying catalysts with optimal descriptor characteristics. While this established approach certainly has *qualitative* merit, its inherent shortcomings (i.e., assumed active site for the reference catalysts, assumed reaction mechanism, intrinsic-errors of DFT functionals, neglect/inadequate treatment of coverage-effects) could potentially lead to predictions that are not *quantitatively* accurate. We propose that: (i) introducing experimental kinetics data to derive the true active site and energetics of the reference catalyst and (ii) using coverage-dependent energetics to on-the-fly update the elementary reaction step's energetics based on the model predicted coverages,[4,6,17] to formulate experiment-calibrated coverage-cognizant volcano plots, could help the community move closer to quantitative accuracy in computational catalyst discovery.

SUMMARY

In this Account, we described an optimization-based mathematically rigorous approach to elucidate the nature of the active site and the reaction mechanism while the catalysis is taking place. We formulate quantitatively accurate MKMs by introducing experimental reaction kinetics data and discussed this methodology for FA decomposition reaction on Au/SiC and Pt/C catalysts. We demonstrated how this approach can be employed to develop high-fidelity MKMs, which can predict the behavior of a catalyst at any experimental condition with quantitative accuracy. Finally,

we highlighted some opportunities for improvement and potential implications of this methodology for computational catalyst discovery.

BIOGRAPHICAL SKETCHES

- Saurabh Bhandari is a Ph.D. student under the supervision of Professor Mavrikakis in the Chemical & Biological Engineering Department at University of Wisconsin-Madison. He received his B.Tech. & M.Tech. in Chemical Engineering from Indian Institute of Technology-Madras. His research focuses on developing detailed MKMs for heterogeneously catalyzed reactions, via a combined computational and experimental approach.
- Srinivas Rangarajan is an Assistant Professor at the Chemical & Biomolecular Engineering Department at Lehigh University. He graduated from Indian Institute of Technology-Madras with a B.Tech in Chemical Engineering. He subsequently obtained his Ph.D. in Chemical Engineering at University of Minnesota, co-advised by Profs. Daoutidis and Bhan. Prior to joining Lehigh, he was a postdoctoral-scholar at University of Wisconsin-Madison, co-advised by Profs. Mavrikakis and Maravelias. His research interests lie in the development of novel computational tools for mechanistic analysis of complex catalytic networks and their application in a variety of chemistries including alkane activation on metal-sulfides, ethylene oxidation on silver, and reversible dehydrogenation of organic hydrogen carriers.
- Manos Mavrikakis is the Paul A. Elfers Professor of Chemical Engineering at the University of Wisconsin-Madison. He received a Diploma in Chemical Engineering from NTUA in Greece, and an MS in Applied Math and PhD in Chemical Engineering & Scientific Computing from the University of Michigan, Ann Arbor. Following postdoctoral work at the University of Delaware and the Technical University of Denmark, he joined the faculty at UW-Madison.

His main research interests include the elucidation of detailed reaction mechanisms for thermal heterogeneously catalyzed and electrocatalyzed reactions and the identification of improved catalytic materials from first principles-based microkinetic modeling. He is the recipient of: the 2009 Paul H. Emmett award in Fundamental Catalysis (North American Catalysis Society), the 2014 R.H. Wilhelm Award in Chemical Reaction Engineering (AIChE), and the 2019 Gabor A. Somorjai Award for Creative Research in Catalysis (ACS). He has been editor-in-chief of the journal *Surface Science* since 2012.

PRESENT ADDRESS

† Present address for Srinivas Rangarajan: Department of Chemical & Biomolecular Engineering, Lehigh University, Bethlehem, PA, 18020, USA

COMPETING INTERESTS

The authors declare that there are no competing interests.

ACKNOWLEDGMENTS

This work was supported by the U.S. Department of Energy – Basic Energy Sciences (DOE-BES), Office of Chemical Sciences, Catalysis Science Program (grant DE-FG02-05ER15731). DFT studies discussed in this article were performed at the National Energy Research Scientific Computing Center, DOE contract DE-AC02-05CH11231. The authors thank Dr. Lang Xu and Ellen Murray for their insightful comments on the manuscript.

REFERENCES

(1) Singh, S.; Li, S.; Carrasquillo-Flores, R.; Alba-Rubio, A. C.; Dumesic, J. A.; Mavrikakis, M. Formic Acid Decomposition on Au Catalysts: DFT, Microkinetic Modeling, and Reaction Kinetics Experiments. *AIChE J.* **2014**, *60*, 1303–1319.

(2) Li, S.; Singh, S.; Dumesic, J. A.; Mavrikakis, M. On the Nature of Active Sites for Formic Acid Decomposition on Gold Catalysts. *Catal. Sci. Technol.* **2019**, *9*, 2836–2848.

(3) Chen, B. W. J.; Stamatakis, M.; Mavrikakis, M. Kinetic Isolation between Turnovers on Au18 Nanoclusters: Formic Acid Decomposition One Molecule at a Time. *ACS Catal.* **2019**, *9*, 9446–9457.

(4) Bhandari, S.; Rangarajan, S.; Maravelias, C. T.; Dumesic, J. A.; Mavrikakis, M. Reaction Mechanism of Vapor-Phase Formic Acid Decomposition over Platinum Catalysts: DFT, Reaction Kinetics Experiments, and Microkinetic Modeling. *ACS Catal.* **2020**, *10*, 4112–4126.

(5) Dumesic, J. A. The Microkinetics of Heterogeneous Catalysis. *ACS Prof. Ref. B.* **1993**.

(6) Grabow, L. C.; Hvolbæk, B.; Nørskov, J. K. Understanding Trends in Catalytic Activity: The Effect of Adsorbate–Adsorbate Interactions for CO Oxidation Over Transition Metals. *Top. Catal.* **2010**, *53*, 298–310.

(7) Jørgensen, M.; Grönbeck, H. First-Principles Microkinetic Modeling of Methane Oxidation over Pd(100) and Pd(111). *ACS Catal.* **2016**.

(8) Nilsson, A.; Pettersson, L. G. M.; Hammer, B.; Bligaard, T.; Christensen, C. H.; Nørskov, J. K. The Electronic Structure Effect in Heterogeneous Catalysis. *Catal. Letters* **2005**, *100*, 111–114.

(9) Cao, L.; Liu, W.; Luo, Q.; Yin, R.; Wang, B.; Weissenrieder, J.; Soldemo, M.; Yan, H.; Lin, Y.; Sun, Z.; et al. Atomically Dispersed Iron Hydroxide Anchored on Pt for Preferential Oxidation of CO in H2. *Nature*. 2019.

(10) Greeley, J.; Mavrikakis, M. Alloy Catalysts Designed from First Principles. *Nat. Mater.* **2004**, *3*, 810–815.

(11) Mavrikakis, M. Computational Methods: A Search Engine for Catalysts. *Nat. Mater.* **2006**, *5*, 847–848.

(12) Medford, A. J.; Vojvodic, A.; Hummelshøj, J. S.; Voss, J.; Abild-Pedersen, F.; Studt, F.; Bligaard, T.; Nilsson, A.; Nørskov, J. K. From the Sabatier Principle to a Predictive Theory of Transition-Metal Heterogeneous Catalysis. *J. Catal.* **2015**, *328*, 36–42.

(13) Yoo, J. S.; Abild-Pedersen, F.; Nørskov, J. K.; Studt, F. A Theoretical Analysis of Transition Metal Catalysts for Formic Acid Decomposition. *ACS Catal.* **2014**, *4*, 1226–1233.

(14) Cheng, J.; Hu, P. Utilization of the Three-Dimensional Volcano Surface to Understand the Chemistry of Multiphase Systems in Heterogeneous Catalysis. *J. Am. Chem. Soc.* **2008**, *130*, 10868–10869.

(15) Bruix, A.; Margraf, J. T.; Andersen, M.; Reuter, K. First-Principles-Based Multiscale Modelling of Heterogeneous Catalysis. *Nat. Catal.* **2019**, *2*, 659–670.

(16) Grabow, L. C.; Mavrikakis, M. Mechanism of Methanol Synthesis on Cu through CO2 and CO Hydrogenation. *ACS Catal.* **2011**, *1*, 365–384.

(17) Grabow, L. C.; Gokhale, A. A.; Evans, S. T.; Dumesic, J. A.; Mavrikakis, M. Mechanism of the Water Gas Shift Reaction on Pt: First Principles, Experiments, and Microkinetic Modeling. *J. Phys. Chem. C* **2008**, *112*, 4608–4617.

(18) Bhan, A.; Hsu, S. H.; Blau, G.; Caruthers, J. M.; Venkatasubramanian, V.; Delgass, W. N. Microkinetic Modeling of Propane Aromatization over HZSM-5. *J. Catal.* **2005**, *235*, 35–51.

(19) Rangarajan, S.; Maravelias, C. T.; Mavrikakis, M. Sequential-Optimization-Based Framework for Robust Modeling and Design of Heterogeneous Catalytic Systems. *J. Phys. Chem. C* **2017**, *121*, 25847–25863.

(20) Wellendorff, J.; Silbaugh, T. L.; Garcia-Pintos, D.; Nørskov, J. K.; Bligaard, T.; Studt, F.; Campbell, C. T. A Benchmark Database for Adsorption Bond Energies to Transition Metal Surfaces and Comparison to Selected DFT Functionals. *Surf. Sci.* **2015**, *640*, 36–44.

(21) Hammer, B.; Hansen, L. B.; Nørskov, J. K. Improved Adsorption Energetics within Density-Functional Theory Using Revised Perdew-Burke-Ernzerhof Functionals. *Phys. Rev. B - Condens. Matter Mater. Phys.* **1999**, *59*, 7413–7421.

(22) Chakarova-Käck, S. D.; Schröder, E.; Lundqvist, B. I.; Langreth, D. C. Application of van Der Waals Density Functional to an Extended System: Adsorption of Benzene and Naphthalene on Graphite. *Phys. Rev. Lett.* **2006**, *96*.

(23) Grabow, L. C.; Mavrikakis, M. Mechanism of Methanol Synthesis on Cu through CO2 and CO Hydrogenation. *ACS Catal.* **2011**, *1*, 365–384.

(24) Christensen, R.; Hansen, H. A.; Vegge, T. Identifying Systematic DFT Errors in Catalytic Reactions. *Catal. Sci. Technol.* **2015**, *5*, 4946–4949.

(25) Mallikarjun Sharada, S.; Bligaard, T.; Luntz, A. C.; Kroes, G. J.; Nørskov, J. K. SBH10: A Benchmark Database of Barrier Heights on Transition Metal Surfaces. *J. Phys. Chem. C* **2017**, *121*, 19807–19815.

(26) Sutton, J. E.; Guo, W.; Katsoulakis, M. A.; Vlachos, D. G. Effects of Correlated Parameters and Uncertainty in Electronic-Structure-Based Chemical Kinetic Modelling. *Nat. Chem.* **2016**, *8*, 331–337.

(27) Matera, S.; Schneider, W. F.; Heyden, A.; Savara, A. Progress in Accurate Chemical Kinetic Modeling, Simulations, and Parameter Estimation for Heterogeneous Catalysis. *ACS Catal.* **2019**, *9*, 6624–6647.

(28) Gokhale, A. A.; Kandoi, S.; Greeley, J. P.; Mavrikakis, M.; Dumesic, J. A. Molecular-Level Descriptions of Surface Chemistry in Kinetic Models Using Density Functional Theory. *Chem. Eng. Sci.* **2004**, *59*, 4679–4691.

(29) Gokhale, A. A.; Dumesic, J. A.; Mavrikakis, M. Article On the Mechanism of Low-Temperature Water Gas Shift Reaction on Copper On the Mechanism of Low-Temperature Water Gas Shift Reaction on Copper. *J. Am. Chem. Soc.* **2008**, *130*, 1402–1414.

(30) Carrasquillo-Flores, R.; Gallo, J. M. R.; Hahn, K.; Dumesic, J. A.; Mavrikakis, M. Density Functional Theory and Reaction Kinetics Studies of the Water-Gas Shift Reaction on Pt-Re Catalysts. *ChemCatChem* **2013**, *5*, 3690–3699.

(31) Rubert-Nason, P.; Mavrikakis, M.; Maravelias, C. T.; Grabow, L. C.; Biegler, L. T. Advanced Solution Methods for Microkinetic Models of Catalytic Reactions: A Methanol Synthesis Case Study. *AIChE J.* **2014**, *60*, 1336–1346.

(32) Demir, B.; Kropp, T.; Rivera-dones, K. R.; Gilcher, E. B.; Huber, G. W.; Mavrikakis, M.; Dumesic, J. A. A Self-Adjusting Platinum Surface for Acetone Hydrogenation. **2019**, 1–5.

(33) Linstrom, P. J.; Mallard, W. G. NIST Chemistry WebBook, NIST Standard Reference Database Number 69. *Natl. Inst. Stand. Technol.* **2014**.

(34) Ojeda, M.; Iglesia, E. Formic Acid Dehydrogenation on Au-Based Catalysts at near-Ambient Temperatures. *Angew. Chemie - Int. Ed.* **2009**, *48*, 4800–4803.

(35) Sachtler, W. M. .; Fahrenfort, J. The Catalytic Decomposition of Formic Acid Vapour on Metals. In *Proceedings of the 2nd International Congress on Catalysis*; Paris (France), 1960; p 831.

(36) Tang, Y.; Roberts, C. A.; Perkins, R. T.; Wachs, I. E. Revisiting Formic Acid Decomposition on Metallic Powder Catalysts: Exploding the HCOOH Decomposition Volcano Curve. *Surf. Sci.* **2016**, *650*, 103–110.

(37) Solymosi, F.; Koós, Á.; Liliom, N.; Ugrai, I. Production of CO-Free H2 from Formic Acid. A Comparative Study of the Catalytic Behavior of Pt Metals on a Carbon Support. *J. Catal.* **2011**, *279*, 213–219.

(38) Gazsi, A.; Bánsági, T.; Solymosi, F. Decomposition and Reforming of Formic Acid on Supported Au Catalysts: Production of CO-Free H2. *J. Phys. Chem. C* **2011**, *115*, 15459–15466.

(39) Zacharska, M.; Chuvilin, A. L.; Kriventsov, V. V.; Beloshapkin, S.; Estrada, M.; Simakov, A.; Bulushev, D. A. Support Effect for Nanosized Au Catalysts in Hydrogen Production from Formic Acid Decomposition. *Catal. Sci. Technol.* **2016**, *6*, 6853–6860.

(40) Bi, Q. Y.; Lin, J. D.; Liu, Y. M.; He, H. Y.; Huang, F. Q.; Cao, Y. Gold Supported on Zirconia Polymorphs for Hydrogen Generation from Formic Acid in Base-Free Aqueous Medium. *J. Power Sources* **2016**.

(41) Ciftci, A.; Ligthart, D. A. J. M.; Pastorino, P.; Hensen, E. J. M. Nanostructured Ceria Supported Pt and Au Catalysts for the Reactions of Ethanol and Formic Acid. *Appl. Catal. B Environ.* **2013**, *130–131*, 325–335.

(42) Sobolev, V.; Asanov, I.; Koltunov, K. The Role of Support in Formic Acid Decomposition on Gold Catalysts. *Energies* **2019**, *12*, 1–8.

(43) Mavrikakis, M.; Stoltze, P.; Nørskov, J. K. Making Gold Less Noble. *Catal. Letters* **2000**, *64*, 101–106.

(44) Williams, W. D.; Shekhar, M.; Lee, W. S.; Kispersky, V.; Delgass, W. N.; Ribeiro, F. H.; Kim, S. M.; Stach, E. A.; Miller, J. T.; Allard, L. F. Metallic Corner Atoms in Gold Clusters Supported on Rutile Are the Dominant Active Site during Water-Gas Shift Catalysis. *J. Am. Chem. Soc.* **2010**, *132*, 14018–14020.

(45) Shekhar, M.; Wang, J.; Lee, W. S.; Williams, W. D.; Kim, S. M.; Stach, E. A.; Miller, J. T.; Delgass, W. N.; Ribeiro, F. H. Size and Support Effects for the Water-Gas Shift Catalysis over Gold Nanoparticles Supported on Model Al2O3 and TiO2. *J. Am. Chem. Soc.* **2012**, *134*, 4700–4708.

(46) Shekhar, M.; Wang, J.; Lee, W. S.; Cem Akatay, M.; Stach, E. A.; Nicholas Delgass, W.; Ribeiro, F. H. Counting Au Catalytic Sites for the Water-Gas Shift Reaction. *J. Catal.* **2012**, *293*, 94–102.

(47) Häkkinen, H. Electronic Shell Structures in Bare and Protected Metal Nanoclusters. *Advances in Physics: X*. 2016.

(48) Miller, S. D.; Kitchin, J. R. Uncertainty and Figure Selection for DFT Based Cluster Expansions for Oxygen Adsorption on Au and Pt (111) Surfaces. In *Molecular Simulation*; 2009.

(49) Han, B. C.; Van Der Ven, A.; Ceder, G.; Hwang, B. J. Surface Segregation and Ordering of Alloy Surfaces in the Presence of Adsorbates. *Phys. Rev. B - Condens. Matter Mater. Phys.* **2005**.

(50) Stamatakis, M.; Piccinin, S. Rationalizing the Relation between Adlayer Structure and Observed Kinetics in Catalysis. *ACS Catal.* **2016**.

(51) Prats, H.; Illas, F.; Sayós, R. General Concepts, Assumptions, Drawbacks, and Misuses in Kinetic Monte Carlo and Microkinetic Modeling Simulations Applied to Computational Heterogeneous Catalysis. *International Journal of Quantum Chemistry*. 2018.

(52) Campbell, C. T. Finding the Rate-Determining Step in a Mechanism: Comparing DeDonder Relations with the "Degree of Rate Control." *J. Catal.* **2001**, *204*, 520–524.

(53) Jia, L.; Bulushev, D. A.; Yu, O.; Boronin, A. I.; Kibis, L. S.; Yu, E.; Beloshapkin, S.; Seryak, I. A.; Ismagilov, Z. R.; Ross, J. R. H. Pt Nanoclusters Stabilized by N-Doped Carbon Nanofibers for Hydrogen Production from Formic Acid. *J. Catal.* **2013**, *307*, 94–102.

(54) Columbia, M. R.; Crabtree, A. M.; Thiel, P. A. Effect of CO on Pt-Catalyzed Decomposition of Formic Acid in Ultrahigh Vacuum. *J. Electroanal. Chem.* **1993**, *345*, 93–105.

(55) Norton, P. R.; Davies, J. A.; Jackman, T. E. Absolute Coverages of CO and O on Pt(111); Comparison of Saturation CO Coverages on Pt(100), (110) and (111) Surfaces. *Surf. Sci.* **1982**, *122*, L593–L600.

(56) Plauck, A.; Stangland, E. E.; Dumesic, J. A.; Mavrikakis, M. Active Sites and Mechanisms for H_2O_2 Decomposition over Pd Catalysts. *Proc. Natl. Acad. Sci. U. S. A.* **2016**, *113*, E1973-82.

(57) Thirumalai, H.; Kitchin, J. R. The Role of VdW Interactions in Coverage Dependent Adsorption Energies of Atomic Adsorbates on Pt(111) and Pd(111). *Surf. Sci.* **2016**, *650*, 196–202.

(58) Biegler, L. T.; Damiano, J. J.; Blau, G. E. Nonlinear Parameter Estimation: A Case Study Comparison. *AIChE J.* **1986**, *32*, 29–45.

(59) Zavala, V. M.; Biegler, L. T. Large-Scale Parameter Estimation in Low-Density Polyethylene Tubular Reactors. *Ind. Eng. Chem. Res.* **2006**, *45*, 7867–7881.

(60) Göltl, F.; Murray, E. A.; Tacey, S. A.; Rangarajan, S.; Mavrikakis, M. Comparing the Performance of Density Functionals in Describing the Adsorption of Atoms and Small Molecules on Ni(111). *Surf. Sci.* **2020**, *700*.

(61) Sprowl, L. H.; Campbell, C. T.; Árnadóttir, L. Hindered Translator and Hindered Rotor Models for Adsorbates: Partition Functions and Entropies. *J. Phys. Chem. C* **2016**.

(62) Jørgensen, M.; Grönbeck, H. Adsorbate Entropies with Complete Potential Energy Sampling in Microkinetic Modeling. *J. Phys. Chem. C* **2017**.

(63) Tian, H.; Rzepa, C.; Upadhyay, R.; Rangarajan, S. Estimating Vibrational and Thermodynamic Properties of Adsorbates with Uncertainty Using Data Driven Surrogates. *AIChE J.* **2019**.

(64) Zafeiratos, S.; Piccinin, S.; Teschner, D. Alloys in Catalysis: Phase Separation and Surface Segregation Phenomena in Response to the Reactive Environment. *Catal. Sci. Technol.* **2012**, *2*, 1787.

(65) Kang, H. C.; Jachimowski, T. A.; Weinberg, W. H. Role of Local Configurations in a Langmuir-Hinshelwood Surface Reaction: Kinetics and Compensation. *J. Chem. Phys.* **1990**, *93*, 1418–1429.

(66) Bligaard, T.; Honkala, K.; Logadottir, A.; Nørskov, J. K.; Dahl, S.; Jacobsen, C. J. H. On the Compensation Effect in Heterogeneous Catalysis. *J. Phys. Chem. B* **2003**, *107*, 9325–9331.

(67) Klimeš, J.; Michaelides, A. Perspective: Advances and Challenges in Treating van Der Waals Dispersion Forces in Density Functional Theory. *Journal of Chemical Physics*. 2012, p 120901.

(68) Hensley, A. J. R.; Ghale, K.; Rieg, C.; Dang, T.; Anderst, E.; Studt, F.; Campbell, C. T.; McEwen, J. S.; Xu, Y. DFT-Based Method for More Accurate Adsorption Energies: An Adaptive Sum of Energies from RPBE and VdW Density Functionals. *J. Phys. Chem. C* **2017**, *121*, 4937–4945.

(69) Walker, E.; Ammal, S. C.; Terejanu, G. A.; Heyden, A. Uncertainty Quantification Framework Applied to the Water-Gas Shift Reaction over Pt-Based Catalysts. *J. Phys. Chem. C* **2016**, *120*, 10328–10339.

(70) Medford, A. J.; Wellendorff, J.; Vojvodic, A.; Studt, F.; Abild-Pedersen, F.; Jacobsen, K. W.; Bligaard, T.; Nørskov, J. K. Assessing the Reliability of Calculated Catalytic Ammonia Synthesis Rates. *Science (80-.).* **2014**, *345*, 197–200.

(71) Sauer, J. Ab Initio Calculations for Molecule-Surface Interactions with Chemical Accuracy. *Acc. Chem. Res.* **2019**, *52*, 3502–3510.

(72) Ou, Q.; Carter, E. A. Potential Functional Embedding Theory with an Improved Kohn-Sham Inversion Algorithm. *J. Chem. Theory Comput.* **2018**, *14*, 5680–5689.

(73) Yu, K.; Carter, E. A. Extending Density Functional Embedding Theory for Covalently Bonded Systems. *Proc. Natl. Acad. Sci. U. S. A.* **2017**, *114*, E10861–E10870.

(74) Pineda, M.; Stamatakis, M. Beyond Mean-Field Approximations for Accurate and Computationally Efficient Models of on-Lattice Chemical Kinetics. *J. Chem. Phys.* **2017**, *147*, 024105.

(75) Bajpai, A.; Frey, K.; Schneider, W. F. Comparison of Coverage-Dependent Binding Energy Models for Mean-Field Microkinetic Rate Predictions. *Langmuir* **2020**, *36*, 465–474.

(76) Abild-Pedersen, F.; Greeley, J.; Studt, F.; Rossmeisl, J.; Munter, T. R.; Moses, P. G.; Skúlason, E.; Bligaard, T.; Nørskov, J. K. Scaling Properties of Adsorption Energies for Hydrogen-Containing Molecules on Transition-Metal Surfaces. *Phys. Rev. Lett.* **2007**, *99*, 4–7.

(77) Nørskov, J. K.; Bligaard, T.; Logadottir, A.; Bahn, S.; Hansen, L. B.; Bollinger, M.; Bengaard, H.; Hammer, B.; Sljivancanin, Z.; Mavrikakis, M.; et al. Universality in Heterogeneous Catalysis. *J. Catal.* **2002**, *209*, 275–278.

CONSPECTUS (DIAGRAM)